

Video Article

Asymmetric Thermoelectrochemical Cell for Harvesting Low-grade Heat under Isothermal Operation

Kaiyu Mu^{*1}, Xun Wang^{*1}, Ka Ho Li¹, Yu-Ting Huang¹, Shien-Ping Feng¹¹Electrochemical Nanoengineering Group, Department of Mechanical Engineering, University of Hong Kong^{*}These authors contributed equallyCorrespondence to: Shien-Ping Feng at hpfeng@hku.hkURL: <https://www.jove.com/video/60768>DOI: [doi:10.3791/60768](https://doi.org/10.3791/60768)

Keywords: Chemistry, Issue 156, thermoelectrochemical cell, low-grade heat, efficiency, graphene oxide, thermo-pseudocapacitive effect, polyaniline

Date Published: 2/5/2020

Citation: Mu, K., Wang, X., Ho Li, K., Huang, Y.T., Feng, S.P. Asymmetric Thermoelectrochemical Cell for Harvesting Low-grade Heat under Isothermal Operation. *J. Vis. Exp.* (156), e60768, doi:10.3791/60768 (2020).

Abstract

Low-grade heat is abundantly available in the environment as waste heat. The efficient conversion of low-grade heat into electricity is very difficult. We developed an asymmetric thermoelectrochemical cell (aTEC) for heat-to-electricity conversion under isothermal operation in the charging and discharging processes without exploiting the thermal gradient or the thermal cycle. The aTEC is composed of a graphene oxide (GO) cathode, a polyaniline (PANI) anode, and 1M KCl as the electrolyte. The cell generates a voltage due to the pseudocapacitive reaction of GO when heating from room temperature (RT) to a high temperature (T_H , ~40-90 °C), and then current is successively produced by oxidizing PANI when an external electrical load is connected. The aTEC demonstrates a remarkable temperature coefficient of 4.1 mV/K and a high heat-to-electricity conversion efficiency of 3.32%, working at a $T_H = 70$ °C with a Carnot efficiency of 25.3%, unveiling a new promising thermoelectrochemical technology for low-grade heat recovery.

Video Link

The video component of this article can be found at <https://www.jove.com/video/60768/>

Introduction

Ubiquitous low-grade heat energy (<100 °C) could be recycled and converted into electricity^{1,2} but is instead wasted. Unfortunately, heat recovery is still a great challenge, because converting low-grade heat to electricity is usually inefficient due to the low temperature differential and the distributed nature of the heat sources³. Intensive research has been conducted in solid-state thermoelectric (TE) materials and devices for the past decades, but the scalable application of TE devices in a low-grade heat regime is limited by the low energy conversion efficiency (η_E) of <2%⁴.

Alternative approaches based on the effect of temperature on electrochemical cells have been suggested as a solution to this problem, because the ionic Seebeck coefficient (α) of thermoelectrochemical cells (TECs) is much higher than that of TE semiconductors^{5,6}. Thermogalvanic cells (TGC) utilize redox active electrolytes sandwiched between two identical electrodes to generate a voltage across the cell when a thermal gradient is applied. The commonly used aqueous $\text{Fe}(\text{CN})_6^{3-}/\text{Fe}(\text{CN})_6^{4-}$ electrolyte in TGCs was reported to have an α of -1.4 mV/K and yield an η_E of <1%^{7,8,9,10,11}. However, TGCs suffer the drawback of the poor ionic conductivity of the liquid electrolyte, which is around three orders of magnitude smaller than the electronic conductivity in TE materials. The electric conductivity could be improved, but this improvement is always accompanied by a higher thermal conductivity, which leads to a lower temperature gradient. Therefore, the η_E of TGCs is inherently limited due to the trade-off between the liquid electrolyte conductance and the temperature requirement for the desired redox reactions in each side of the electrode.

A thermally regenerative electrochemical cycle (TREC)^{12,13,14} based on a battery system using a solid copper hexacyanoferrate (CuHCF) cathode and a Cu/Cu^+ anode was recently reported. TREC is configured as a pouch cell to improve the electrolyte conductance, showing an α of -1.2 mV/K and reaching a high η_E of 3.7% (21% of η_{Carnot}) when operated at 60 °C and 10 °C. Nevertheless, one limit of TREC is that external electricity is required at the start of the process to charge the electrodes in each thermal cycle, leading to complicated system designs¹⁴. A TREC without this limitation can be achieved, but it suffers from a poor conversion efficiency of <1%¹³. The TREC system demonstrates that a sodium-ion secondary battery (SIB)-type thermocell consisting of two types of Prussian blue analogues (PBA) with different α values can harvest waste heat. The thermal efficiency (η) increases proportionally with ΔT . Moreover, η reaches 1.08%, 3.19% at $\Delta T = 30$ K, 56 K separately. The thermal cyclability is improved using Ni-substituted PBA^{15,16,17,18}.

Alternatively, a thermally regenerative ammonia battery (TRAB) employs copper-based redox couples $[\text{Cu}(\text{NH}_3)_4]^{2+}/\text{Cu}$ and $\text{Cu}(\text{II})/\text{Cu}$ that operate with the reverse temperature gradient by switching the temperature of electrolyte co-operated with positive and negative electrodes,

which produces a η_E of 0.53% (13% of η_{Carnot}). However, this system is configured with two tanks full of liquid electrolyte, causing sluggish heating and cooling. Also, the ammonia stream in the system creates concerns regarding safety, leakage, and stability^{19,20,21}.

Here we present an asymmetric thermoelectrochemical cell (aTEC) for heat-to-electricity conversion that can be thermally charged and electrically discharged by continuous isothermal heating without maintaining a temperature gradient in a geometric configuration or switching temperatures in a thermal cycle. The aTEC uses asymmetric electrodes, including a graphene oxide (GO) cathode and a polyaniline (PANI) anode, and KCl as the electrolyte. It is thermally charged via the thermo-pseudocapacitive effect of GO and then discharged with the oxidation reaction of PANI. Notably, the aTEC exhibits a high α of 4.1 mV/K and attains a η_E of 3.32%, the highest ever achieved at 70 °C (25.3% of η_{Carnot}).

Protocol

1. Preparation of the graphene oxide electrode

- Synthesis of graphene oxide via the modified Hummer's method
 - Steps 1.1.2 and 1.1.3 occur at a low temperature (<0 °C). Circulate ice water flowing through the external layer of a double wall glass beaker placed on a magnetic stirrer to create low temperature conditions for the reactants inside.
 - Mix 1 g of sodium nitrate (NaNO₃) with 100 mL of sulfuric acid (H₂SO₄, reagent grade, 95-98%) using slow stirring in the beaker.
 - Add 1 g of flake graphite into the sulfuric acid and stir for 1 h in the cold bath. Add 6 g of potassium permanganate (KMnO₄) gradually to the solution and stir the mixture for another 2 h.
 - The next step of the reaction takes place at a middle temperature (~35 °C). Change the ice water to 35 °C water and continue the oxidation of the graphite by stirring for ½ h.
 - The last step of the reaction takes place at a T_H (80-90 °C). Add 46 mL of deionized (DI) water (70 °C) into the reaction tank drop by drop. Note that that the reaction is strong. Add 140 mL of DI water and 20 mL of hydrogen peroxide (30% H₂O₂) in the reaction tank as the last step of the reaction. Make sure that golden particles of GO appear as a result.
 - Wash the product thoroughly with dilute hydrochloric acid (HCl) and DI water several times until the GO suspension reaches pH = 7.
 - Freeze the washed GO suspension overnight and dry it in a freeze dryer until water evaporates completely.
- Preparation of the graphene oxide electrode
 - Mix the graphene oxide, carbon black, and PVDF in a mass ratio of 75:15:10 and put them in a glass bottle. Drip the solvent N-methyl-2-pyrrolidone (NMP) into the solid mixture and ensure the weight ratio of solvent and solid mixture is 4:1.
 - Prepare the paste by mixing at 2,000 rpm for 13 min and defoaming in 1,200 rpm for 2 min with a mixer.
 - Brush coat the paste on carbon paper until the coat is ~8-15 mg/cm² and dry it for 4 h at 40 °C.

2. Preparation of the polyaniline (PANI) electrode

- Prepare 1 wt% carboxymethyl cellulose (CMC) aqueous solution by dissolving CMC powder in DI water by stirring for 10 h.
- Mix 50 mg of leucoemeraldine-base PANI and 10 mg of carbon black in a beaker. Add 150 μ L of 1 wt% CMC solution into the beaker and mix with a magnetic stirrer for 12 h.
- Add 6 μ L of 40% styrene-butadiene (SBR) solution into the mixture and stir for another 15 min.
- Place a piece of carbon paper on the doctor blade coater and drop the mixed PANI slurry at the leading edge of the carbon paper.
- Blade coat the slurry to produce a film 400 μ m thick on the carbon paper. Dry the coating for 4 h at 50 °C.

3. Assembling the pouch cell

- Cut titanium foil into the appropriate size and then connect each piece to a nickel tab with a 20 kHz ultrasonic spot welding machine.
- Place the porous hydrophilic polypropylene-based separator between the GO electrode and the PANI electrode to avoid short circuits. Each electrode is paired with one current collector.
- Package the electrodes using aluminum laminated film. Seal the sides of the aluminum laminated film with a compact vacuum sealer for 4 s. Set the temperature of the top and bottom sealing parts as 180 °C and 160 °C separately.
- Inject 500 μ L of the 1 M KCl electrolyte into the pouch cell and allow to equilibrate for 10 min.
- Extrude the excess electrolyte and seal the last side of the pouch cell in a -80 kPa vacuum chamber.

4. Setting up the temperature controlling system

- Stack the pouch cell between two thermoelectric modules. Place thermocouples on the top and bottom sides of the cell. Apply thermal paste to all the interfaces to ensure good thermal contact.
NOTE: The temperature is controlled with LabVIEW code. Temperatures measured from the thermocouples are compared with the setting temperatures and the output voltage is determined by the difference between the real time temperature and setting temperature via a PID control. The voltage signals are transmitted to the power supply and are connected to the thermoelectric module. The closed-loop control guarantees a temperature measurement accuracy within ± 0.5 °C.

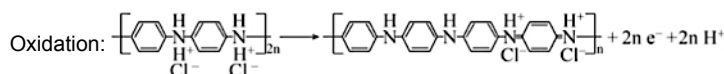
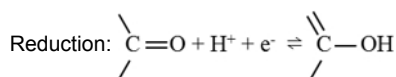
5. Electrochemical characterization

1. Perform the electrochemical tests of the cell using a potentiostat. Conduct the thermal charging in open circuit mode while carrying out the electrical discharging process at a constant current.

Representative Results

The aTEC pouch cell was configured with asymmetric electrodes consisting of a GO cathode, a PANI anode, and filled with the KCl electrolyte. The thickness of the pouch cell shown in **Figure 1A** is 1 mm, which facilitates isothermal conditions between the two electrodes as well as efficient heat conduction. The scanning electron microscopy (SEM) images of the GO cathode and the PANI anode coated on carbon paper are shown in **Figure 1B** and **Figure 1C**. The porous structure increases the contact area between the active electrode materials and the electrolyte, thus optimizing the discharging current and the output power.

With the different work functions of the asymmetric electrodes, a built-in voltage (ΔV_0) was observed on the cell in open circuit conditions at RT (**Figure 2A₁**). When aTEC was heated from RT to T_H , heat triggered the pseudocapacitive reactions between functional groups containing oxygen (e.g., C=O bonds) and protons in the electrolyte at the GO-aqueous interface, thus the cell voltage (V_{oc}) increased as electrons moved to the surface of the GO (**Figure 2A₂**). When an external load was connected, the aTEC was discharged under the potential differential between electrodes at T_H , where the discharge capacity was mainly due to the oxidation of the PANI anode and the reduction of functional groups (**Figure 2A₃**), which can be presented as



The voltages of aTEC during thermal charging and electrical discharging at $T_H = 70^\circ\text{C}$ are shown in **Figure 2B**. The open circuit potential reached 0.185 V when the cell was heated from RT to $T_H = 70^\circ\text{C}$, where aTEC exhibited a high temperature coefficient ($\alpha = \partial V/\partial T$, where V is the electrode voltage and T is the temperature) of 4.1 mV/K. The discharging of aTEC was conducted under a constant current of 0.1 mA. The specific gravimetric capacity of the GO was 10.43 mAh/g while that of the PANI was 103.4 mAh/g. The heat-to-electricity conversion efficiency of aTEC can be calculated as the output electrical work (W) divided by input thermal energy, which can be expressed as

$$\eta_E = \frac{W}{Q_H + Q_{iso}} = \frac{\int V dq}{(1 - \eta_{HX}) \sum m C_p \Delta T + T_H \Delta S}$$

The output electrical work was calculated from the integration of discharging voltage over charge capacity while the input thermal energy consisted of the Q_H for heating the cell up from RT to T_H and Q_{iso} for heat absorbed during discharging at T_H . In the equation, q is the discharge capacity, η_{HX} is the efficiency of heat recovery, m is the mass of the active materials of electrodes and electrolyte, C_p is the specific heat, ΔT is the temperature difference between the operating temperature and RT, and ΔS is the reaction entropy change. Based on the discharging shown in **Figure 2B**, our aTEC attained a η_E of 3.32% at 70°C , which is equivalent to 25.3% of η_{Carnot} (13.1%).

The isothermal operating of aTEC allows its use in many various scenarios. The aTEC can be charged by a hot pot with boiling water (**Figure 3**). The voltage of six aTECs connected in a series can reach >1 V. Our aTEC illustrated an excellent heat-to-electricity performance with a high temperature coefficient and energy conversion efficiency. The cell device performance and operating temperature window could be further improved by changing the composition of the electrolyte and using electrode materials with high α , low heat capacity, and robust functionalities. Our work sheds light on the design of thermoelectrochemical systems. With further research and development, aTEC has the potential to become a key technology for low-grade heat recovery.

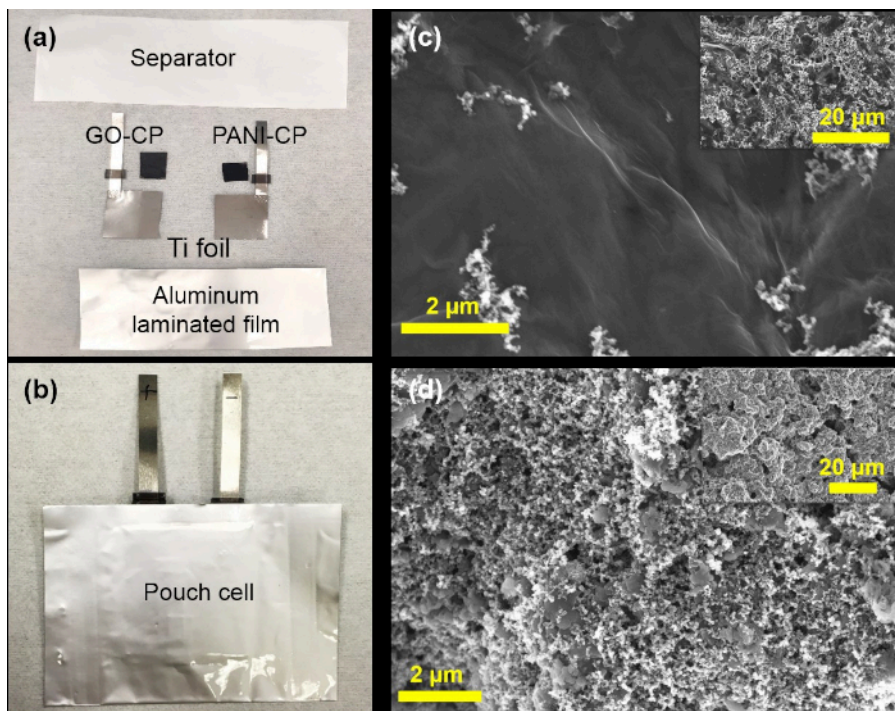


Figure 1: aTEC pouch cell. (A) Pouch cell configuration. The GO cathode and the PANI anode are assembled with the titanium (Ti) foil current collector and separated by the hydrophilic polypropylene separator. SEM images of (B) the GO cathode and (C) the PANI anode both coated on carbon paper. [Please click here to view a larger version of this figure.](#)

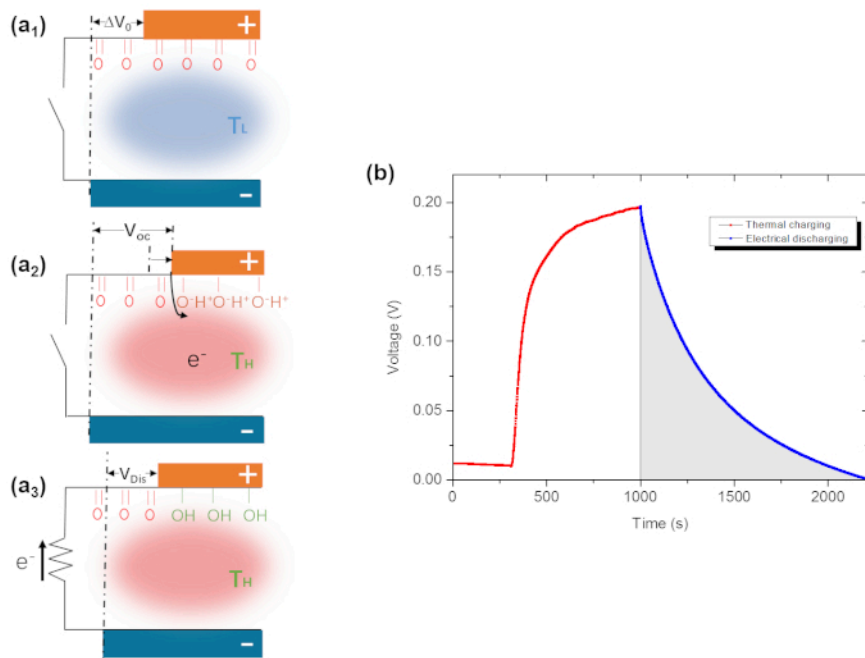


Figure 2: aTEC charging and discharging. (A) Working principle of aTEC. (B) Open circuit voltage of the thermal charging process (red line) and electrical discharging curve (blue line) of the aTEC. [Please click here to view a larger version of this figure.](#)



Figure 3: Demonstration of aTEC charged by a hot pot. [Please click here to view a larger version of this figure.](#)

Operating mode	TEC system	Structure and Materials	a	η_E	Ref
			(mV/K)	(η_E/η_{Carnot})	
Temperature gradient (continuous operation based on the temperature-dependent redox potentials at the hot and cold sides)	TGC	Electrode: Multi-walled carbon nanotubes (MWCNT) based electrode	1.4	0.24%	9
		Electrolyte: $K_3Fe(CN)_6/K_4Fe(CN)_6$		-1.40%	
	TGC	Electrode: Carbon-based material	1.85	0.11%	6
		Electrolyte: $K_3[Fe(CN)_6]/(NH_4)_4[Fe(CN)_6]$ or $Fe_2(SO_4)_3/FeSO_4$		-0.40%	
	TGC	Electrode: CNT aerogel sheets	1.43	0.55%	8
		Electrolyte: $K_3Fe(CN)_6/K_4Fe(CN)_6$		-3.95%	
Temperature gradient	RFB	Electrode: carbon cloth	3	1.80%	10
		Flow electrolyte: $[Fe(CN)_6]^{3-}/[Fe(CN)_6]^{4-}$ and V^{3+}/V^{2+}		-15%	
Temperature cycle	TREC	Electrode: CuHCF and Cu	1.2	3.70%	14
		Electrolyte: $NaNO_3$ and $Cu(NO_3)_2$		-25%	
	TREC	Electrode: NiHCF and Ag/AgCl	0.74	1.60%	12
		Electrolyte: KCl		-13%	
	TREC	Electrode: $KFe^{II}Fe^{III}(CN)_6$ and $K_3Fe(CN)_6/K_4Fe(CN)_6$ with carbon cloth	1.45	0.72%	13
		Electrolyte: KNO_3		-6.00%	
	TRAB	Electrode: Cu	-	0.86%	19
		Electrolyte: $Cu(NO_3)_2/NH_4NO_3$		-6.10%	
Electrode: Cu		0.70%		20	
Flow electrolyte: $Cu(NO_3)_2/NH_4NO_3$	-5.00%				
Temperature cycle	aTEC	Electrode: GO and PANI	4.1	3.32% (25.3%)	This work
		Electrolyte: KCl			

Table 1: Comparison of different TEC technologies for low-grade heat-to-electricity conversion.

Discussion

The aTEC converts thermal energy into electricity via a thermal charging process when heating from RT to T_H and a successive electrical discharging process at T_H . Getting rid of the dependence on a temperature gradient or a temperature cycle like the TGC and TREC, aTEC allows isothermal heating operation during the entire charging and discharging processes. Thermal induced voltage is based on the pseudocapacitive effect of GO because heating facilitates the chemisorption of protons on the oxygen functional groups of GO, causing the pseudocapacitive reaction at the GO-aqueous interface. PANI contributes little to the increased voltage but provides electrons in the discharging process. The utilization of the KCl electrolyte keeps the charge of the electrode-electrolyte interface balanced during the reaction and improves the conductivity of the whole cell. The system is nontoxic and environmentally friendly, which makes it ideal for commercial applications. Other

alternatives for the electrolyte can be chloride salt, such as NaCl, because chloride ions play an essential role in the oxidation reaction of PANI in the discharging process.

Unlike technologies based on thermal gradients or thermal cycles, aTEC is unique and has potential for practical applications due to its low cost, flexibility, light weight, its isothermal and continuous thermal charge/electrical discharge process, and the ability to form stacks of cells. The aTEC achieves a high α of 4.1 mV/K and a high ηE of 3.32% (equivalent to 25.3% of η_{Carnot}) at 70 °C, which is superior to existing techniques for low-grade heat harvesting. A comparison of aTEC and other TEC techniques is shown in **Table 1**.

The cyclability performance of aTEC is still unsatisfactory. This may be improved by adding a redox couple into the electrolyte or changing the electrode materials. Prussian blue analogs (PBA) are likely to make a better anode electrode for aTEC, because the negative temperature coefficient of some PBAs can help enhance the efficiency of aTEC. An aTEC with improved cyclability has great potential for commercial use, such as recovering waste heat from an air conditioner.

Disclosures

The authors declare no competing financial interests.

Acknowledgments

The authors acknowledge constructive discussion with Prof. D.Y.C. Leung and Dr. Y. Chen (The University of Hong Kong), Prof. M.H.K. Leung (City University of Hong Kong), Dr. W. S. Liu (Southern University of Science and Technology), and Mr. Frank H.T. Leung (Techskill [Asia] Limited). The authors acknowledge the financial support of General Research Fund of the Research Grants Council of Hong Kong Special Administrative Region, China, under Award Number 17204516 and 17206518, and Innovation and Technology Fund (Ref: ITS/171/16FX).

References

1. Chu, S., Majumdar, A. Opportunities and Challenges for A Sustainable Energy Future. *Nature*. **488**, 294 (2012).
2. Forman, C., Muritala, I. K., Pardemann, R., Meyer, B. Estimating the Global Waste Heat Potential. *Renewable and Sustainable Energy Reviews*. **57**, 1568-1579 (2016).
3. Gur, I., Sawyer, K., Prasher, R. Searching for A Better Thermal Battery. *Science*. **335** (6075), 1454-1455 (2012).
4. He, R., Schierning, G., Nielsch, K. Thermoelectric Devices: A Review of Devices, Architectures, and Contact Optimization. *Advanced Materials Technologies*. **3** (4), 1700256 (2018).
5. Abraham, T. J., MacFarlane, D. R., Pringle, J. M. High Seebeck Coefficient Redox Ionic Liquid Electrolytes for Thermal Energy Harvesting. *Energy & Environmental Science*. **6** (9), 2639-2645 (2013).
6. Zhang, L. et al. High Power Density Electrochemical Thermocells for Inexpensively Harvesting Low-Grade Thermal Energy. *Advanced Materials*. **29** (12), 1605652 (2017).
7. Duan, J. et al. Aqueous Thermogalvanic Cells with A High Seebeck Coefficient for Low-Grade Heat Harvest. *Nature Communications*. **9** (1), 5146 (2018).
8. Im, H. et al. High-Efficiency Electrochemical Thermal Energy Harvester Using Carbon Nanotube Aerogel Sheet Electrodes. *Nature Communications*. **7**, 10600 (2016).
9. Hu, R. et al. Harvesting Waste Thermal Energy Using A Carbon-Nanotube-Based Thermo-Electrochemical Cell. *Nano Letters*. **10** (3), 838-846 (2010).
10. Poletayev, A. D., McKay, I. S., Chueh, W. C., Majumdar, A. Continuous Electrochemical Heat Engines. *Energy and Environmental Science*. **11** (10), 2964-2971 (2018).
11. Qian, W., Li, M., Chen, L., Zhang, J., Dong, C. Improving Thermo-Electrochemical Cell Performance by Constructing Ag-MgO-CNTs Nanocomposite Electrodes. *RSC Advances*. **5** (119), 97982-97987 (2015).
12. Lee, S. W. et al. An Electrochemical System for Efficiently Harvesting Low-Grade Heat Energy. *Nature Communications*. **5**, 3942 (2014).
13. Yang, Y. et al. Charging-Free Electrochemical System for Harvesting Low-Grade Thermal Energy. *Proceedings of the National Academy of Sciences*. **111** (48), 17011-17016 (2014).
14. Yang, Y. et al. Membrane-Free Battery for Harvesting Low-Grade Thermal Energy. *Nano Letters*. **14** (11), 6578-6583 (2014).
15. Fukuzumi, Y., Amaha, K., Kobayashi, W., Niwa, H., Moritomo, Y. Prussian Blue Analogues as Promising Thermal Power Generation Materials. *Energy Technology*. **6** (10), 1865-1870 (2018).
16. Shibata, T., Fukuzumi, Y., Kobayashi, W., Moritomo, Y. Thermal Power Generation During Heat Cycle Near Room Temperature. *Applied Physics Express*. **11** (1), 017101 (2018).
17. Shibata, T., Fukuzumi, Y., Moritomo, Y. Thermal Efficiency of A Thermocell Made of Prussian Blue Analogues. *Scientific Reports*. **8** (1), 14784 (2018).
18. Takahara, I., Shibata, T., Fukuzumi, Y., Moritomo, Y. Improved Thermal Cyclability of Tertiary Battery Made of Prussian Blue Analogues. *ChemistrySelect*. **4** (29), 8558-8563 (2019).
19. Zhang, F., Liu, J., Yang, W., Logan, B. E. A Thermally Regenerative Ammonia-Based Battery for Efficient Harvesting of Low-Grade Thermal Energy as Electrical Power. *Energy and Environmental Science*. **8** (1), 343-349 (2015).
20. Zhu, X., Rahimi, M., Gorski, C. A., Logan, B. A Thermally-Regenerative Ammonia-Based Flow Battery for Electrical Energy Recovery from Waste Heat. *ChemSusChem*. **9** (8), 873-879 (2016).
21. Zhang, F., LaBarge, N., Yang, W., Liu, J., Logan, B. E. Enhancing Low-Grade Thermal Energy Recovery in a Thermally Regenerative Ammonia Battery Using Elevated Temperatures. *ChemSusChem*. **8** (6), 1043-1048 (2015).